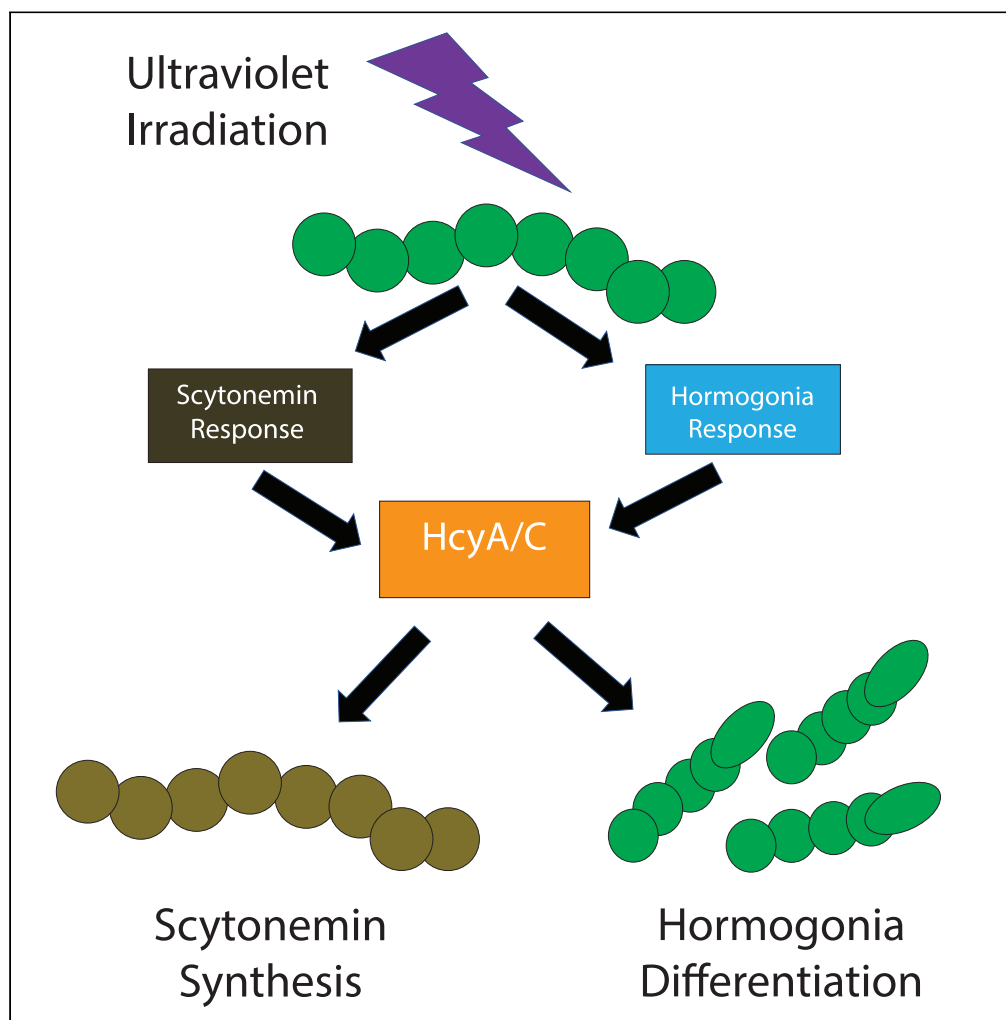


Article

A regulatory linkage between scytonemin production and hormogonia differentiation in *Nostoc punctiforme*

Kevin Klicki,
Daniela Ferreira,
Douglas Risser,
Ferran Garcia-
Pichel

ferran@asu.edu

Highlights

Nostoc responds to UV-A by both producing sunscreen and differentiating hormogonia

The responses are, however, mutually exclusive at the single filament level

A novel 4-gene system (*hcyA-D*) orchestrates the regulation between the two responses

This affords *Nostoc* a bet-hedging means to both hunker down and flee UV-A stress

Klicki et al., iScience 25,
104361
June 17, 2022 © 2022 The
Author(s).
[https://doi.org/10.1016/
j.isci.2022.104361](https://doi.org/10.1016/j.isci.2022.104361)

Article

A regulatory linkage between scytonemin production and hormogonia differentiation in *Nostoc punctiforme*Kevin Klicki,^{1,2} Daniela Ferreira,² Douglas Risser,³ and Ferran Garcia-Pichel^{1,2,4,*}

SUMMARY

Bacteria sometimes hedge their survival bets by concurrently activating response circuits leading to different phenotypes in isogenic populations. We show that the cyanobacterium *Nostoc punctiforme* responds to UV-A by concurrently producing the sunscreen scytonemin and differentiating into motile hormogonia but segregating the responses at the filament level. Mutational studies show that a four-gene partner-switching regulatory system (*hcyA-D*) orchestrates the cross-talk between the respective regulatory circuitries. Transcription of hormogonium genes and *hcyA-D* is upregulated by UVA through the scytonemin two-component regulator (*scyTCR*), *hcyA-D* being directly involved in signal transduction into the hormogonium response and its modulation by visible light. The sigma factor cascade that regulates developmental commitment to hormogonia also upregulates *hcyA-D* transcription and strongly suppresses scytonemin synthesis through downregulation of the *scyTCR* itself. Through this complex bidirectional mechanism, *Nostoc* can concurrently deploy two fundamentally different UV stress mitigation strategies, either hunker down or flee, in a single population.

INTRODUCTION

Organisms in nature are subject to a wide range of often concurrent environmental stressors, and in response, adaptive strategies for sensing and responding to these environmental challenges have evolved at both the molecular and cellular levels. The classical paradigm of environmental stress response in bacteria consists of a molecular circuit that modulates cellular activity by exerting transcriptional, post-transcriptional, or post-translational control over processes relevant to the environmental stimulus (Gao and Stock, 2009; Magasanik, 1961). This model implies a one-to-one relationship between stress factor and stress response. In reality, even genetically identical populations of bacteria can exhibit phenotypic heterogeneity in response to a uniform environmental stimulus and yield differing responses from individual cells by a combination of genetically programmed and stochastic mechanisms (Ackermann, 2015; Smits et al., 2006). One evolutionary strategy that exploits phenotypic heterogeneity to increase population fitness is bet-hedging, wherein phenotypic diversity in an isogenic population allows for the population as a whole to enhance its combined probability of survival to environmental fluctuations that may be either too rapid to be addressed by genetic regulation, or for which the maintenance of separate, dedicated signal transduction systems would be too costly (Beaumont et al., 2009; Levy et al., 2012). This approach may be particularly useful to an organism subject to a simultaneous barrage, or a rapidly oscillating variety of environmental stressors (Ackermann, 2015; Holland et al., 2014a). A range of molecular mechanisms leading to phenotypic variation in an isogenic population have been identified that can be epigenetic, stochastic, and cell-cycle-based in nature (Avery, 2006; Raj and van Oudenaarden, 2008). Importantly, as subpopulations commit to diverging responses, they must regulate cellular functions in a manner consequent with that commitment.

Among microbes, cyanobacteria are particularly prone to radiative environmental insults in that their photosynthetic metabolism exposes them by necessity to solar radiation (Whitton and Potts, 2012). Many cyanobacteria are dominant in habitats characterized by high insolation (Potts, 1994; Revsbech and Jorgensen, 1983; van Gemerden, 1993), in which exposure to UV radiation (UVR) can bring about significant collateral damage, and have thus developed a suite of adaptations to mitigate its deleterious effects, including DNA and protein repair, behavioral avoidance of exposure by migration patterns, the

¹Center for Fundamental and Applied Microbiomics, Biodesign Institute, Arizona State University, Tempe, AZ 85281, USA

²School of Life Sciences, Arizona State University, AZ 95281, USA

³Department of Biological Sciences, University of the Pacific, Stockton, CA 95211, USA

⁴Lead contact

*Correspondence: ferran@asu.edu

<https://doi.org/10.1016/j.isci.2022.104361>



synthesis of antioxidants, or the production of UV-absorbing sunscreens (Rastogi et al., 2014; Singh et al., 2010). While some of these seem to be universal among cyanobacteria, like DNA damage repair or specific replacements of the D1 protein in photosystem II (Rastogi et al., 2014), some are of restricted distribution. Only some cyanobacteria, for example, can produce the sunscreen scytonemin (Garcia-Pichel and Castenholz, 1991), a brownish-yellow lipid-soluble sunscreen that accumulates in the extracellular polysaccharide layer in response to UV-A (315–400 nm) exposure (Gao and Garcia-Pichel, 2011). This response is regarded as a passive adaptation particularly useful in cyanobacteria that endure periods of quiescence (Soule et al., 2007). By contrast, active behavioral responses based on photophobic responses to UV have only been described for filamentous, non-heterocystous cyanobacteria like *Oscillatoria* spp. (Nadeau et al., 1999) and *Microcoleus* spp. (Bebout and Garcia-Pichel, 1995). These two types of adaptations would seem to be mutually exclusive given this ecological niche separation. In other words, either the organisms hunker down and endure the insults, or they flee. *Nostoc punctiforme* has become the model organism to study scytonemin, as it is the only producer that is genetically tractable. Although *N. punctiforme* is sessile (i.e., non-motile) in its vegetative life stage, it is also capable of motility responses after undergoing a developmental cycle to form hormogonia, which are specialized short filaments that are characteristically motile and buoyant and that serve as a means for colony dispersal. Fluctuating nutrient or salt concentrations, diminishing light intensity, or the presence of symbiotic partners (Meeks et al., 2002) will all elicit in *N. punctiforme* the genetic expression patterns that lead to differentiation of motile hormogonia, which will “glide” to an area more conducive to growth and promptly de-differentiate into sessile primordia, and eventually into colonial vegetative forms (Meeks et al., 2002; Risser et al., 2014; Soule et al., 2009a). In general, the genus *Nostoc* is widely distributed in the terrestrial environment, from Antarctic valleys to arid deserts (Dodds et al., 1995), where it is often found as a symbiont to a variety of plants and fungi (Dodds et al., 1995; Meeks et al., 2001). During the establishment of symbiosis, *N. punctiforme* will differentiate into hormogonia in response to nutrient conditions and/or plant secondary messengers (Campbell et al., 2008; Ekman et al., 2013).

Gene expression for both types of adaptations in *Nostoc* is tightly controlled. In the case of scytonemin, a canonical (Rajeev et al., 2011) two-component regulatory system (henceforth the scytonemin TCR or scyTCR) directly controls its downstream polycistronic biosynthetic operon (Soule et al., 2009b). The scyTCR is essential for scytonemin production (Naurin et al., 2016), and its histidine kinase contains chromophore-binding motifs; while the chromophore is unknown, it is likely responsible for sensing its environmental stimulus, UV-A radiation. Hormogonia differentiation requires several disparate cellular functions to work in concert, including a specialized type IV pilus system that provides the primary motive force to carry filaments along (Khayatan et al., 2015), gas vesicles to provide buoyancy in aqueous environments (Armstrong et al., 1983), the production of specific polysaccharide, as well as genes involved in reductive cell division such as *ftsZ* and *ftsY* (Gonzalez et al., 2019). Most of the hormogonia-related genes are co-regulated by a tripartite hierarchical sigma factor cascade (Gonzalez et al., 2019), consisting of sigma factors J, F, and C, that chaperone the RNA polymerase to their transcriptional targets (Davis et al., 2017).

Because UV-A radiation exposure in *Nostoc* can elicit a large number of presumably adaptive responses beyond scytonemin synthesis (Soule et al., 2013) for which the regulatory components are unknown, we began a survey of regulatory targets of the scytonemin TCR by RNA sequencing of scytonemin TCR deletion mutants under the hypothesis that its regulatory capacity might be more general than previously thought. Surprisingly, these analyses provided evidence for a regulatory cross-talk between hormogonia differentiation and scytonemin synthesis, which we explore further in this contribution.

MATERIALS AND METHODS

Strains and culture conditions

Mutant construction

In-frame deletion mutants Δ Reg, Δ RR, Δ sigJ, Δ hcyA, and Δ hcyC were generated from their respective parent strain (*N. punctiforme* UCD 153 for Δ Reg and Δ RR, *N. punctiforme* ATCC 29133 for Δ sigJ, Δ hcyA, and Δ hcyC) by homologous recombination as described in Cai and Wolk (1990). (Table 1) PCR primers were designed to amplify DNA upstream and downstream of the desired deletion site (1.0 kb–3.0 kb on each side) and containing overlapping sequences (Cai and Wolk, 1990; Cohen et al., 1994) (Table S1). PCR products were checked and cloned into carrier plasmid pRL278. Plasmids were introduced into the wild type by conjugation, and selected by a combination of antibiotic and sucrose counter selection markers, as explained in detail in the study by Gonzalez et al., (2019).

Phenotypic characterization

Scytonemin induction assays. Scytonemin production was induced by growing the strains in 15 × 100 mm glass Petri dishes under white light at 50 $\mu\text{mol photons m}^{-2}\text{s}^{-1}$ supplemented with a UV-A flux of 7.5 $\mu\text{mol photons m}^{-2}\text{s}^{-1}$ supplied by black-light fluorescent bulbs (General Electric) for 5 days at 21°C. For some experiments, as noted where applicable, white light was omitted. Scytonemin production was detected by microscopic observation first, using a Carl Zeiss AxioScope.A1 at 100× magnification and by HPLC on a Waters e2695 equipped with a Supelco Discovery HS F5-5 column connected to a Waters 2998 PDA UV-Vis diode array detector as described in the study by Klicki et al., (2018).

Standard Hormogonia induction assays. Hormogonia induction was carried out following the study by Khayatan et al., (2015): *Nostoc* strains were streaked onto agar-solidified medium supplemented with 5% sucrose and grown heterotrophically in the dark until punctate colonies formed. Colonies were then transferred to agar-solidified media lacking sucrose and exposed to 10 $\mu\text{mol photons m}^{-2}\text{s}^{-1}$ provided at a 90-degree angle. Formation of hormogonia was detected visually under the dissection scope. Plate motility assays were performed as previously described (Khayatan et al., 2015). This assay yields a massive differentiation involving the large majority of existing filaments.

Hormogonia/scytonemin co-induction was carried out on solid AA medium using aluminum foil-wrapped glass Petri plates provided with a side window, where the foil had been cut out, so that white light could enter at a 90-degree angle at an intensity of 10 $\mu\text{mol photons m}^{-2}\text{s}^{-1}$. UV-A radiation was concurrently delivered from a 2 cm^2 top window that allowed for the entirety of the colony to be exposed to UV-A, after passing through a 400 nm cut-off short-pass optical filter (Edmund Optics) to remove any visible light produced by the UV-A bulbs. This was necessary because we found in pilot experiments that any additional vertically supplied visible light from the UV bulbs inhibited standard phototactic hormogonia induction. For analyses, scytonemin/hormogonia co-induction cultures were transferred from agar plates to microscope slides using a scalpel and photographed on a Carl Zeiss AxioScope.A1 at 1000× magnification using an AxioCam 105 color camera. They were inspected for morphologically identifiable hormogonia, and for the typical extracellular coloration imparted by scytonemin. UV-A exclusive hormogonia induction was carried out by plating strains from liquid cultures on to solid AA medium and incubating under UV-A irradiation without supplemental PAR for 48–96 h. Hormogonia spreading was quantified by measuring the area occupied by initial colony biomass and the area swept out by whisks of hormogonia using the Carl Zeiss Zen 3.1 software, subtracting the former from the latter, and dividing the difference by the initial biomass area. The absence of scytonemin in actively differentiated hormogonia was demonstrated by collecting cellular populations enriched in hormogonia as well as the vegetative colony from which they had radiated and extracting lipid soluble pigments in 100% acetone from each, respectively. Extracts were analyzed for the presence of scytonemin by HPLC as previously described. The scytonemin to chlorophyll a ratio as evidenced by HPLC peak area for three replicates of UV-A-induced hormogonia and vegetative cells as well as uninduced vegetative cells were compared via student's T-tests. The enrichment of hormogonia versus vegetative cells in either population was verified microscopically by performing width measurements for 200 cells from each.

UV phototaxis induction was carried out on solid AA medium with wild type and mutant colonies supplied with UV-A irradiation through a short pass filter at a 25-degree angle. Directional colony spreading was observed microscopically.

Environmental fitness of *N. punctiforme* 29,133, ΔhcyA , and ΔhcyC was assessed by plating cells onto the center of a Petri dish filled with sterilized sandy desert soil and subjecting them to exclusive UV-A irradiation for 48 h. Plates were then moved to standard light conditions and hydrated periodically with sterilized water. Plates were photographed after 3 weeks of growth under standard light conditions.

RNA extraction, sequencing, and RNAseq analyses

Total RNA was extracted from appropriately incubated cultures (UV-A-induced or uninduced) of each test strain (wild type, ΔRR , and ΔReg) using previously described methods (Campbell et al., 2007a). Ribodepletion, cDNA synthesis, and subsequent RNA sequencing were performed at the Arizona State University Genomics Facility as follows. Four μg of total RNA was submitted to ribodepletion using the MICROBExpress Bacterial mRNA Enrichment Kit (Ambion). Directional cDNA libraries were synthesized using rRNA-depleted samples. Three libraries per strain were multiplexed and treatments sequenced independently

on an Illumina NextSeq 500 using a v2 2x75 pair end kit sequenced generating 76 base pair reads, obtaining on average $9,773,321 \pm 5,550,035$ reads per sample, excluding 16 and 23S rRNA genes. Sequences were aligned and assembled to the *Nostoc punctiforme* PCC 73102 genome using Rockhopper (Tjaden, 2015) on default parameters independently for each replicate. Differential expression between mutants and UV treatments was calculated using the DEseq algorithm in Rockhopper (Tjaden, 2015). Given the roughly 6,000 non-rRNA genes in the *N. punctiforme* genome, only transcripts whose differential expression had a q-value (a false discovery rate corrected p value) of less than 10^{-15} were considered significant for downstream analyses. Contiguous genes of known function that exhibited similar degrees of differential expression were considered to be co-regulated. Reads per kilobase million for each gene from the Rockhopper output were square root transformed to accentuate expressional differences over a broader dynamic range. Heatmaps were constructed using Pheatmap (Kolde and Antoine, 2015)

Targeted analysis by RT-qPCR

Five-hundred ng of total RNA was used to synthesize cDNA using the Protoscript first-strand cDNA synthesis kit and random hexamer primers (New England Biolabs) according to manufacturer's protocols. 1 μ L of resulting cDNA was used as qPCR template. Transcripts were amplified using primer sets targeting specific genes as described in Table S1, using an ABI 7900 HT Real-time PCR system and PerfeCTa SYBR Fastmix according to manufacturer's protocols. Transcript level was quantified in three technical replicates of each treatment using the $2^{-\Delta\Delta CT}$ method with expression normalized relative to *rnpB* as previously done by Gonzalez et al., (2019), and results averaged per treatment.

Bacterial adenylate cyclase two-hybrid assays

The bacterial adenylate cyclase two-hybrid assay (BACTH) was employed to probe protein-protein interaction between HcyC (Npun_F1684) and HcyA (Npun_F1682) with the putative phosphorylated serine residues replaced with alanine, as well as sigma factors C, F, and J. To construct a plasmid-encoding HcyC fused to the T25 fragment of *Bordetella pertussis* adenylate cyclase for bacterial adenylate cyclase two-hybrid (BACTH) analysis (Battesti and Bouveret, 2012; Karimova et al., 1998), the coding region gene was amplified via PCR and cloned into pKT25 as an XbaI-KpnI fragment using restriction sites introduced on the primers. BTH101 (adenylate cyclase-deficient) *Escherichia coli* strains transformed with appropriate plasmids were streaked onto Lysogeny Broth (LB) agar plates containing 100 μ g/mL Ampicillin and 50 μ g/mL Kanamycin, and incubated at 30 °C for 48 h. For each strain, 1 mL of LB containing 100 μ g/mL Ampicillin, 50 μ g/mL Kanamycin, and 0.5 mM Isopropyl β -D-1-thiogalactopyranoside (IPTG) was inoculated with several colonies from the plate, and cultures were then incubated overnight at 30°C with shaking at 230 rpm. Subsequently, 2 μ L were taken from each overnight culture and spotted onto MacConkey agar plates containing 100 μ g/mL Ampicillin and 50 μ g/mL Kanamycin. Plates were incubated at 30°C for 48 h prior to imaging.

RESULTS

Patterns in RNAseq expression analysis

The original intent of the present study was to identify ancillary regulatory targets of the scytonemin TCR. To this end, RNA sequencing was conducted on *N. punctiforme* UCD 153 (wild type) and derived scytonemin TCR (scyTCR) system mutants ΔRR lacking the AraC-type DNA-binding transcription factor that controls expression of the scytonemin operon and ΔReg lacking the putative UV-A-sensing PAS domain containing sensor histidine kinase, both under UV-A inductive conditions and in the absence of UV (non-induced). The expectations were that any genes under control of this TCR would show a relative downregulation in the mutants, and that the differences would be dependent on inductive (UV-A exposed) conditions. We found that out of the 6219 ORFs in the genome, 527 were statistically differentially expressed ($q < 10^{-15}$) between wild type and either one of the two regulatory mutants under scytonemin-inductive conditions (Figure 1 and S2). Most of this response was seen in the double mutant rather than in the response regulator mutant, consistent with the crucial role of the histidine kinase in the photosensory response. Under non-inductive conditions, the number of differentially expressed ORFs between wild type and mutants was reduced by more than half, but not completely abolished, indicating that the scytonemin TCR can also exert regulatory control based on non-UV-A sensory inputs. Unexpectedly, we found a large group of genes (207 under UV-A induction and 132 in its absence) that were more intensely expressed in ΔReg than in the wild type. While most of these genes were annotated as hypothetical, one contiguous cluster (Npun_F0198 to Npun_F0237) included a heat shock protein HSP20, UV damage endonuclease, and

Interestingly, the *ebo* gene cluster (Npun_R5231–Npun_F5236), which is essential for the synthesis of scytonemin as an intermediary export system to the periplasm (Klicki et al., 2018), did not exhibit differential expression between wild type and scytonemin TCR mutants (data available through NCBI SRA accession PRJNA728749), despite being demonstrably induced by UV-A exposure (Soule et al., 2009a). Thus, the *ebo* operon in *Nostoc* is likely under the control of a separate photoregulatory system.

Three other functional gene clusters (Figure 1) displayed conspicuous differential downregulation in the TCR mutants: one encoding gas vesicle proteins, another one, just downstream of it, coding for a variety of chemotaxis-related proteins (Npun_F2147 to Npun_F2164) and the *pilM-Q* cluster (Npun_F5005 to Npun_F5008) encoding type IV pilus system components (Gonzalez et al., 2019). All of these clusters are typically and exclusively expressed in *Nostoc* during the development of hormogonia. The level of wild-type expression for these clusters under UV-A induction was 3- to 4-fold higher than that in the uninduced wild-type cultures, showing that UV-A did play an inductive role in their expression. However, while the *scy* genes were downregulated very strongly (some 200-fold), these went down only by 5- to 6-fold with *scyTCR* deletion.

Finally, expression of a 4-gene cluster of putative, but unspecified, regulatory function (Npun_F1682–Npun_R1685) was also negatively affected by the deletion of the scytonemin TCR (2- to 3-fold; $q = 10^{-15}$) under conditions of UV-A induction. This effect was not detected in uninduced cultures ($q > 0.4$), indicating that the *scyTCR* has a UV-A-dependent role in the promotion of their expression in the wild type, similar to the canonical effect on the scytonemin operon. Differential expression levels, however, were more in line with those seen in the hormogonia-related genes discussed above (Figure 1). The cluster contains a gene predicted to be an anti-sigma factor antagonist (henceforth *hcyA*), followed by a RsbU-like phosphatase (henceforth *hcyB*), an anti-sigma factor (henceforth *hcyC*), and a multi-sensor hybrid histidine kinase (henceforth *hcyD*).

UV-A as an environmental cue for hormogonia development

The preceding results showing the positive regulation by *scyTRC* of expression of typical hormogonia genes suggest that UV-A may function as an environmental cue to their differentiation. But no such reports existed in the literature. To test this, we exposed cultures of the wild type to standard UV-A radiation fluxes in the dark (i.e., with no visible light). Abundant hormogonia developed within a few days (Figure 2), whereas no hormogonia developed in controls without UV. However, if as little as $5 \mu\text{mol m}^{-2} \text{s}^{-1}$ of visible light was included in the assays, no hormogonia developed. While it is clear that UV-A acts as a stimulus of hormogonia development, their motility showed no phototactic directionality toward or away from UV (Figure S3).

Involvement of the *hcyA-D* cluster in UV-mediated hormogonia differentiation

The RNAseq results suggested that the scytonemin TCR may be responsible for a regulatory linkage between scytonemin production and hormogonia differentiation within the frame of a higher-order regulatory network, wherein the *hcyA-D* genes may be the key to this linkage. To probe for UV-A-dependent hormogonia-related phenotypes associated with these genes, in frame deletion knockouts ($\Delta hcyA$ and $\Delta hcyC$) were constructed. Indeed, $\Delta hcyA$ displayed a decrease in hormogonia differentiation capacity relative to wild-type *N. punctiforme* (Figure 2) under UV induction assays, whereas $\Delta hcyC$ showed no such inhibition, while no significant effect on hormogonia differentiation under standard inductive conditions was observed between mutants (Figure S4). When screened for scytonemin production in standard UV-A induction assays, both $\Delta hcyA$ and $\Delta hcyC$ were positive and showed no difference in accumulation compared to their wild-type counterpart (Figure S5). These results are consistent with the notion that HcyC acts as an inhibitor of the hormogonium cascade so that its absence would not bring about a decrease in hormogonia differentiation, and that HcyA acts as an HcyC inhibitor whose absence would allow HcyC to inhibit the process more strongly. To test if these two putative regulatory elements could be part of a coordinated system, we conducted bacterial two-hybrid tests, which confirmed that HcyA and HcyC can physically interact *in vivo* (Figure S5), adding evidence beyond their genomic location that HcyC is a target of HcyA activity. As was seen in the wild type, addition of visible light at low intensity could suppress the UV-A-induced development of hormogonia in the $\Delta hcyC$ mutant, but unlike in the wild type, exposure to high fluxes of visible light restored the response. This restoration by high light was not detected in $\Delta hcyA$.

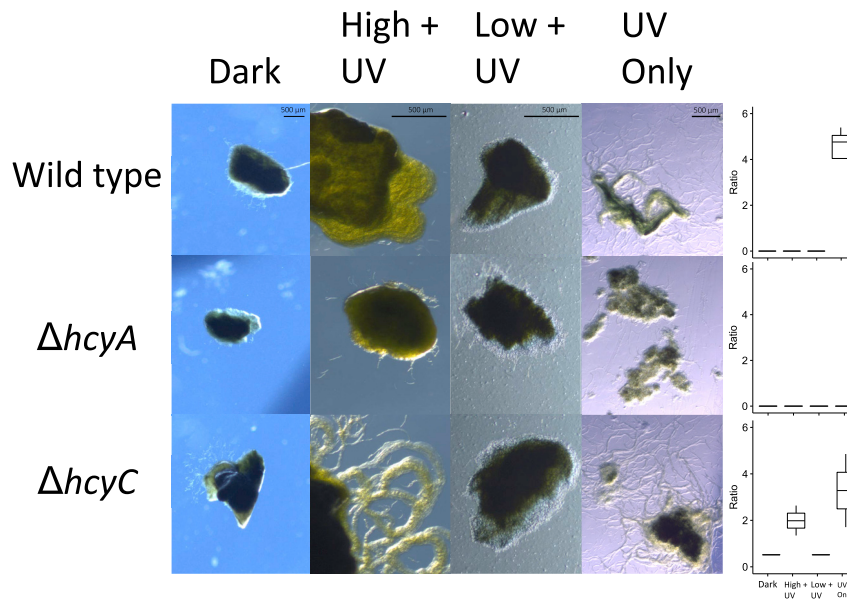


Figure 2. Phenotypic responses of wild type, $\Delta hcyA$, and $\Delta hcyC$ after 5 days in dark, high light ($100 \mu\text{mol m}^{-2} \text{s}^{-1}$) + UV, low light ($10 \mu\text{mol m}^{-2} \text{s}^{-1}$) + UV, and dark + UV conditions

Hormogonia can be seen spreading from the central clump of vegetative cells in wild type and $\Delta hcyC$ in UV-only conditions, but not in $\Delta hcyA$, while they can be seen emanating only from $\Delta hcyC$ under high light + UV conditions. Boxplots represent hormogonium spreading quantification for each mutant and condition (see materials and methods) of 3 independent colonies. The experiment was repeated three times independently with qualitatively identical results.

Surprisingly, two-hybrid interaction screens of HcyC against SigC, SigF, and SigJ (the sigma factors whose regulon controls hormogonia differentiation) did not yield any evidence of protein-protein interaction suggesting that the target of HcyC's activity is a different sigma factor or regulatory element altogether (Figure S6). Overall, the results implicate the hcyA-D regulatory system in the hormogonium differentiation regulatory cascade elicited by UV-A, rather than in the scytonemin regulatory system.

Suppression of scytonemin synthesis in hormogonia under UV-A

To examine regulatory interactions in the reverse direction (i.e., the hormogonium regulatory cascade acting on the scytonemin regulation), we conducted experiments with *N. punctiforme* ATCC 29133 and its derived sigma factor regulatory mutants in which hormogonia formation was induced with the standard phototactic assay, but with concurrent exposure to UV radiation. Cells were exposed to visible light laterally, and UV-A radiation from above. After five days, cultures were examined microscopically. We could determine that scytonemin had been produced in all wild type as well as $\Delta hcyA/C$ strains, and concurrently, hormogonia had formed in all strains (Figure 4). Deletion mutants did thus not interfere with scytonemin formation under phototactic induction, as they did not under UV induction (see above), and both responses proceeded concurrently. However, we noticed a clear populational segregation in the responses. In all cases, only a small part of the *Nostoc* filaments had differentiated into hormogonia, and those that did, did not exhibit the characteristic extracellular brownish coloration of scytonemin. Conversely, scytonemin production occurred only in the subpopulation that remained in the vegetative state (Figures 3 and 4). These findings confirm the notion that hormogonia differentiation and scytonemin production cannot proceed simultaneously in a single filament and indicate that a regulatory mechanism must be at play to suppress scytonemin production once a cell is committed to differentiation, even under concurrent UV-A irradiation. The mechanism of this functional segregation cannot be reliant on the hcy system, however, as populations of hcy deletion mutants showed identical phenotypic heterogeneity to wild type.

We re-examined the RNAseq time course conducted by Gonzalez et al., (2019) in which expression changes were followed during the process of phototactic hormogonium differentiation paying particular attention to changes in expression of scytonemin-related genes under standard phototactic hormogonia induction. Expectedly, because the cultures were not exposed to UV, neither scytonemin nor ebo operons displayed

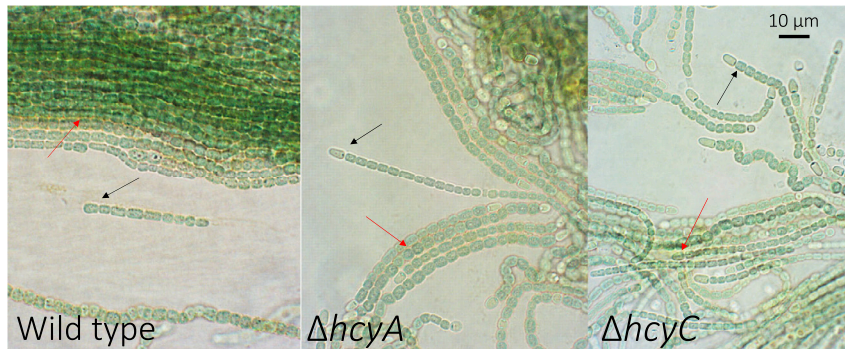


Figure 3. Co-induction of scytonemin production and hormogonia differentiation in wild type, $\Delta hcyA$, and $\Delta hcyC$ mutants

Scytonemin can be seen as a brownish yellow sheath accumulating around vegetative cells, but not around hormogonia in all three strains. Black arrows point to hormogonium filaments and red arrows point to extracellular scytonemin accumulation in each frame. Quantitative assessment of scytonemin production is in [Figure S3](#).

any significant changes in expression. However, the histidine sensor kinase of the scyTCR was down-regulated 7-fold during this 24-h time course ([Figure 5](#)), essentially blinding to UV-A any cells committed to develop into hormogonia. In a parallel analysis of the sigma factor J regulatory mutant, no such downregulation of the scytonemin histidine kinase was observed over the same time course ([Figure 6](#)) indicating that sigma factor J is, directly or indirectly, responsible for this suppression. The Gonzalez transcriptome also revealed expression of *hcyA* and *hcyC* to be dependent on sigma factor C ([Gonzalez et al., 2019](#)). The expression of sigma factor C is itself directly dependent on sigma factor J ([Gonzalez et al., 2019](#)), thus deletion of sigma factor J has the effect of abolishing phototactic induction of *hcyA-C* ([Figure 6](#))

Dynamics of UV-A mediated upregulation of scytonemin and hormogonia responses

Two reasons prompted us to inspect more closely the induction of the hormogonia response genes that we saw with the RNAseq data in [Figure 1](#) under conditions of scytonemin induction (UV-A in the presence of visible light). First, scytonemin production in response to UV-A takes place over a period of 4–6 days ([Soule et al., 2009a](#)) while the typical phototactic hormogonia differentiation takes only 24 h ([Gonzalez et al., 2019](#)). Second, the fact that induction, although statistically significant, did demonstrably not lead to an actual, phenotypically detectable formation of hormogonia ([Figure 2](#)). For this, we conducted an RT-qPCR-based time course analysis of relevant genes. We chose hormogonia gas vesicle protein A (*gvpA*, Npun_F2159) and type IV pilus assembly protein (*pilM*, Npun_F5005) to represent the hormogonia response. The analyses were carried out with the wild-type strains and the scyTCR and sigma factor regulatory mutants under standard scytonemin induction conditions over a period of 120 h. The results ([Figure 6](#)) corroborated the RNAseq data in that a clear induction by 5 days was seen in *pilM* and *gvpA* genes in the wild type, but not in ΔRR or ΔReg . This induction was, however, dynamically much more sluggish and less intense than that seen under phototactic induction of hormogonia differentiation (compare with [Figure 6](#)). The involvement of the *hcy* system in this induction was also patent in that $\Delta hcyA$ mutants failed to respond. Interestingly, $\Delta hcyC$ mutants had a short-lived peak of expression during the first day, while both wild type and all other mutants showed a relative expression decrease early on. These results are consistent with the presence of competing sensory signals and regulatory systems: one that can induce the hormogonia genes based on the UV-A signals, and another one repressing these genes through other inputs (possibly visible light, see [Figure 2](#)) in which HcyC participates, given that its absence allows their expression at least during the early response.

To determine if the HcyA-D partner switching system imparts a fitness advantage in *Nostoc*'s natural environment, wild type, $\Delta hcyA$, and $\Delta hcyC$ were inoculated on sterilized soil and subjected to UV irradiation. As predicted from UV-induced motility from agar plates, $\Delta hcyC$ displayed the emergence of satellite colonies 2–3 weeks after UV irradiation, while $\Delta hcyA$ displayed none ([Figure S7](#)).

DISCUSSION

RNAseq analyses of deletion mutants in the scyTCR of *Nostoc punctiforme* demonstrated that the suite of genes under its influence is much more diverse than previously considered, that it includes both up- and

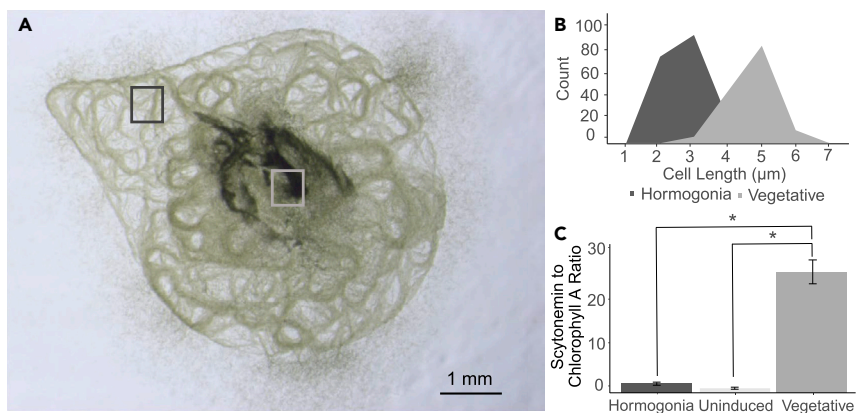


Figure 4. Cellular and molecular differentiation of vegetative and hormogonia populations of UV-irradiated cultures

(A) Representative image of a typical colony exhibiting UV-induced hormogonia differentiation with central colony highlighted with light gray box and hormogonia highlighted with dark gray box (B) Cell size distribution in colony (light gray) and hormogonia (dark gray) populations. Hormogonia cells undergo reductive cell division during differentiation, resulting in the distribution of cell sizes to be left skewed, while vegetative cell populations exhibited a larger average cell size.

(C) Ratio of scytonemin to chlorophyll a in hormogonia and vegetative cell populations as determined by HPLC analysis of separated population extracts. Hormogonia showed minimal accumulation of scytonemin compared to vegetative cells.

downregulation of various genes and multigene loci, and that it likely also incorporates sensory inputs other than UV-A radiation. It apparently downregulates at least some genes involved in photooxidative stress responses alternative to scytonemin production. In its regulon, the most puzzling targets were sets of genes presumably involved in the development of hormogonia, the meaning of which we pursued in this contribution.

Bet-hedging in response to UV-A exposure

Our experiments demonstrate that the segregation between motility and sunscreen responses to UV-A (i.e., the choice between hunkering down and passively enduring its stress vs. actively fleeing), both of which were known from different species of cyanobacteria (Castenholz and Garcia-Pichel, 2007), have an intra-populational parallel in a single species genetically capable of both types of responses. Our work demonstrated that UV-A cues in themselves suffice to elicit hormogonia differentiation in *Nostoc*, concurrently with the well-known synthesis of scytonemin (Soule et al., 2009a). However, the responses were mutually exclusive at the cellular level, as *Nostoc* hormogonia failed to produce scytonemin even in the presence of UV-A radiation levels that elicited its synthesis in cells of the same original population that had remained in the vegetative state.

In terms of populational fitness, it may well make sense for *Nostoc* to hedge its bets by deploying both types of responses concurrently. This may ensure a higher rate of survival under ultraviolet stress of unknown magnitude, as sunscreens may or may not provide sufficient protection under harsh regimes, and hormogonia are not guaranteed a safe journey to more benign settings. This strategy of risk spreading in the face of fluctuating environmental conditions is known as bet-hedging (De Jong et al., 2011). Maintaining genetically encoded phenotypic heterogeneity may be of particular utility in the face of unpredictably fluctuating environmental conditions (Ackermann, 2015). These points were further supported by experiments that sought to recreate *Nostoc*'s natural soil environment. The absence of components in the Hcy system that enable this bet-hedging strategy caused fewer satellite colonies to emerge after a period of UV-A irradiation followed by desiccation, suggesting that a small proportion or none of the original population were able to differentiate into hormogonia during UV-A stress (Figure 4). The crux is how to manage regulatory stress responses for both types of adaptations in a coordinated manner. In other words, how to obtain the desired heterogeneity in response first, and then how to silence the alternative pathway once a commitment is made at the cellular level. The first part of the problem is not very different from the choices faced by *Nostoc* populations under stressors other than UV-A, in that differentiation of hormogonia is

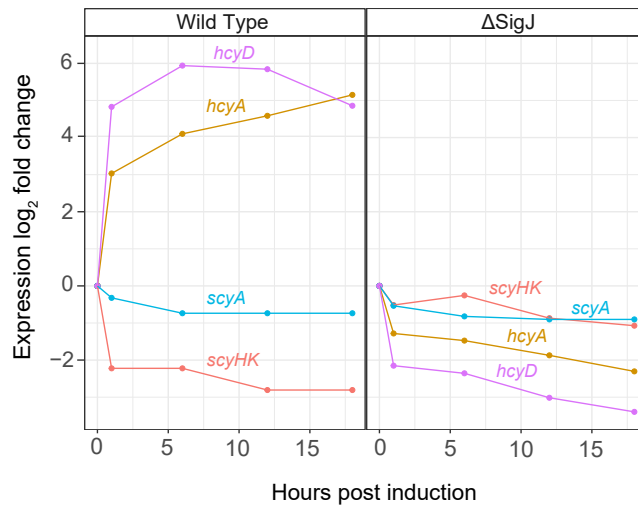


Figure 5. Expression of scytonemin biosynthetic (*scyA*) and regulatory (*scyHK*) genes, as well as *hcyA* and *hcyD*, over a phototactic hormogonium induction time course (raw data from Gonzalez et al., 2019) for the wild type and $\Delta sigJ$ deletion mutant. Expression levels are relative to those in wild type at time 0. The *scyT* TCR histidine kinase is downregulated during phototactic hormogonium induction in the wild type, but not in $\Delta sigJ$. Genes in the *hcyA-D* system show the opposite effect.

apparently generally not universal, except under controlled laboratory conditions (Splitt and Risser, 2016), and only portions of the natural population will commit to the developmental pathway (Campbell et al., 2008). Many instances of phenotypic response heterogeneity have been observed across bacteria (Ackermann, 2015), suggesting that a diversity of stress responses in a clonal population can increase overall fitness in the face of fluctuating environmental stressors (Holland et al., 2014b). The presence of double-negative, imbricated regulatory systems (McCaw et al., 2002; Schurr et al., 1993; Smits et al., 2006), as well as transcriptional noise and stochasticity (Ackermann, 2015) are thought to play a key role in the generation of phenotypic response heterogeneity. A conspicuous case of phenotypic heterogeneity occurs in cyanobacteria during nitrogen fixation, wherein a small subset of cells in an isogenic population modulate expression of nitrogenase components based on a circadian clock (Adams, 2000; Mohr et al., 2013). The basic mechanism that allows phenotypic heterogeneity to arise under UV-A may well be intrinsic to the core hormogonia regulatory cascade (Figure 7), although the specifics are neither known nor easily derived from current knowledge. Our research provides some mechanistic insights into a means for coordination and cross-talk between the two canonical regulatory pathways involved.

How and why hormogonia suppress scytonemin synthesis

The regulatory basis of this phenomenon can be traced to the downregulation of the *scyTCR* expression by sigma J, as demonstrated by the $\Delta sigJ$ knockouts during phototactic hormogonium differentiation (Figure 3). The extent of this downregulation in committed hormogonia is in fact not fully encompassed by the populational RNAseq data, in that a 6- to 7-fold downregulation signal stemming from a just a portion of cells (committed hormogonia under the present UV-A inductive conditions) that may make up at most some 10% of the population, implies that the single-cell downregulation effect in hormogonia themselves could be close to an order of magnitude higher, although the precise experimental conditions used may influence this proportion, as standard phototactic assays yield near 100% differentiation of hormogonia. In any event, this downregulation of the *scyTCR* likely denies hormogonia the ability to respond to UV-A cues that would otherwise strongly upregulate scytonemin genes. Although the specific mechanism of this transcriptional repression cannot be directly discerned from our data, it is unlikely that sigma J acts directly as a repressor of the *scyTCR* transcription because sigma factors promote expression by recruiting RNA polymerase to their target transcriptional start site (Helmann and Chamberlin, 1988; Wösten, 1998). Sigma J may in turn upregulate the expression of a putative secondary transcriptional repressor that targets the scytonemin TCR locus. This regulatory separation makes sense in terms of energetics of investment, in that any scytonemin formed by hormogonia would be exported to the extracellular polysaccharide layer, and thus be left behind as they glide away from it, negating any potential beneficial effects to the

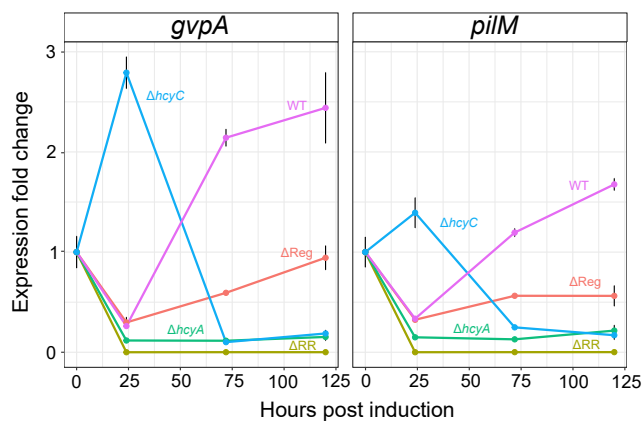


Figure 6. Expression changes relative to time 0 of hormogonia-associated genes *gvpA* and *pilM* in wild type (WT), Δ RR, Δ Reg, Δ hcyA, and Δ hcyC mutants under standard scytonemin inductive conditions (UV-A plus white light) over 120 h. Both genes showed increased expression over the time course in the wild type, but no such induction in Δ RR, Δ Reg, or Δ hcyA. Δ hcyC showed a burst of early upregulation but decreased to low levels after the first day.

hormogonium. The investment in an ineffective sunscreen would add to the already burdened metabolism of hormogonia differentiation, which involves the cessation of vegetative metabolic activities in exchange for overproduction of hormogonia-specific proteins (Marsac, 1994).

UV-A can elicit hormogonia differentiation and this response is modulated by visible light

Our results point to the *hcyA-D* quadripartite regulatory system as a crucial link between the canonical scytonemin and hormogonia regulatory cascades (Figure 7). On the one hand, as a unit, its expression was enhanced by the UV-A-sensing scyTCR (Figure 1), and mutants of one of its components, *hcyA*, failed to develop hormogonia under induction by UV-A (Figure 2), both linking its expression to the scytonemin circuit. On the other hand, it is overexpressed during phototactic hormogonia differentiation in a process dependent on the master regulator of the hormogonia cascade, sigma J (Figure 6). Additionally, expression of some of its genes is controlled by members of the tripartite hierarchical sigma factor cascade (sigma factors J, F, and C) (Gonzalez et al., 2019). Notably, we found no differential expression or phenotypic effects of the *hcy* deletion mutants on the scytonemin systems, indicating that its main ultimate regulatory target is hormogonia differentiation. These results clearly link the system to the canonical hormogonia regulatory circuitry. Interestingly, the *hcyA-D* cluster is conserved in sequence homology of its components and genomic architecture only among a small group of cyanobacterial genomes corresponding to genera that are capable of differentiating hormogonia and producing scytonemin (*Nostoc*, *Calothrix*, and *Tolypothrix*), but not in other cyanobacteria, which speaks for adaptations to UV beyond *Nostoc* itself.

Furthermore, this system is also at least partly responsible for the integration of visible light signals that can demonstrably counteract the induction of the hormogonium circuit by UV-A. HcyC seems to play a role in this signal integration as its deletion mutant was unable to carry out fully the suppression of UV-A-induction mediated by (high intensity) visible light (Figure 2) and displays a differential early burst of hormogonia gene expression (Figure 6).

While the precise mechanisms of the *hcyA-D*-mediated interaction cannot be directly determined from our data, bioinformatic examination may provide some insights. The system contains four genes, three of which are annotated as potential components of a partner-switching regulatory unit, including a putative anti-sigma factor (*hcyC*), an anti-sigma factor antagonist (*hcyA*), and a phosphatase (*hcyB*), and we demonstrate that *hcyC* and *hcyA* interact physically *in vivo* (Figure S4). The multi-sensor hybrid histidine kinase encoded by *hcyD* (Npun_R1685) contains two GAF domains and one PAS sensory similarly to *scyHK* according to the NCBI Conserved Protein Domain Database (Marchler-Bauer et al., 2011, 2015, 2017). The former is known to be a chromophore-binding domain (Wagner et al., 2005), suggesting that it may play a photosensory role (Wiltbank and Kehoe, 2019), and in fact *hcyD*'s GAF domain contains twin cysteine residues (C833

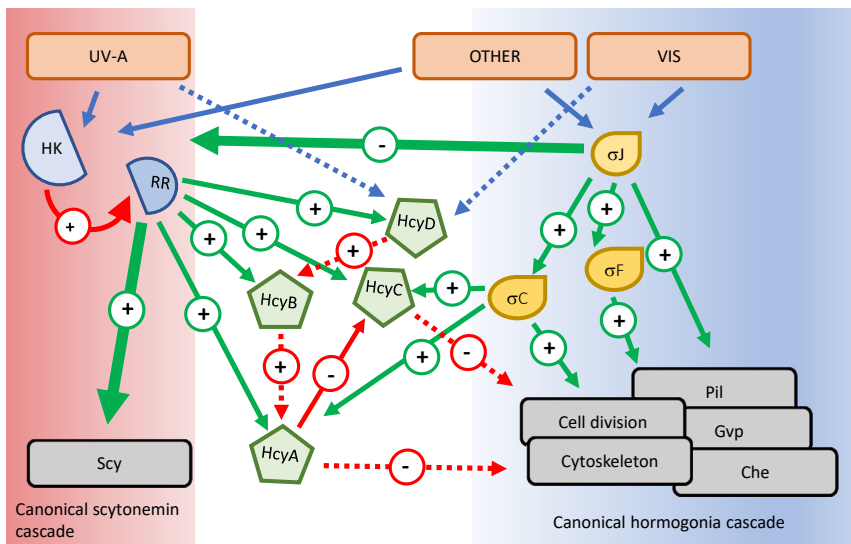


Figure 7. Working model of the scytonemin-hormogonium gene regulatory network. The extent of the canonical networks for each is shown over colored background. Cross-talk of the canonical systems is enabled by the one-way repression by sigma factor J over the scytonemin TCR on the one hand, and by the *hcyA-D* partner switching system on the other, which receives transcriptional controls from both canonical networks but exerts control over the hormogonia genes only. Orange rectangles and blue arrows represent input signals. Gray boxes represent functional outputs. Green arrows denote transcriptional control, and red lines represent post-translational control. Solid lines represent demonstrated interactions, and dotted lines represent suspected or deduced interactions. Positive and negative signs refer to the respective type of interaction.

and C841) which were shown to bind a UV-sensing chromophore in UirS of *Synechocystis* PCC 6803 (Song et al., 2011). *hcyD*'s histidine kinase domain may activate other components of the *hcy* system; however, unlike the GAF domain-containing UirS UV sensor kinase of *Synechocystis* PCC 6803 (Song et al., 2011), *hcyD* does not elicit a photophobic directionality to hormogonia motility (Figure S3). By analogy to similar partner-switching systems, a potential candidate is the phosphatase HcyB, with homology to RsbU (Delumeau et al., 2004), which is known in *Bacillus subtilis* to be activated by a sensor kinase, and in turn dephosphorylates an anti-sigma factor antagonist (Delumeau et al., 2004). By analogy, HcyB could dephosphorylate HcyA, relieving its inhibition of HcyC. Similarly, one might be inclined to postulate the *hcyA-D* system exerts its control over the expression of hormogonia development through post-translational interactions between HcyC and Sigma J. However, it is clear from two-hybrid analyses that HcyC does not directly interact with any of the three hormogonia-related sigma factors *in vivo*. If HcyC were to actually act as an anti-sigma factor, the target would have to be found outside of the canonical tripartite cascade. However, other studies have found that similar partner-switching systems, such as HmpWUV in *N. punctiforme*, can have final output effects on non-sigma factor targets (Mercer and Lang, 2014; Morris and Visick, 2013; Riley et al., 2018). This could well be the case with *hcyA-D* given that a lack of *hcyA* led to a complete loss of UV-A-induced hormogonia formation as shown in Figure 4, suggesting that HcyC is inhibiting some regulatory element that positively affects hormogonia development. In the $\Delta hcyC$ mutant background, HcyA has no target to inhibit, and thus hormogonia differentiation proceeds unabated.

It is also possible that the apparent complexity in regulatory circuitry may contribute to the process of populational bifurcation in the phenotypic responses to UV-A, since negative feedback loops similar to the regulatory mechanism that mediates it, directly lead to cases of phenotypic heterogeneity (McCaw et al., 2002; Schurr et al., 1993; Smits et al., 2006). In the present working model (Figure 7), sigma factor J indirectly and negatively regulates the scytonemin TCR and indirectly and positively regulates expression of the *hcyA-D* system, which in turn negatively regulates, directly or indirectly, hormogonia responses.

Limitations of study

Clearly, further experimentation will be needed to characterize the components, precise interactions, and phenotypic outcomes of this complex gene regulatory network to the point of gaining a sound mechanistic

Table 1. *Nostoc punctiforme* strains utilized in this work

| Strain | Description | Mutation Locus Tag | Function | Mutant Phenotype |
|---------------------|---|---------------------------|---|--|
| ATCC 29133 | Wild Type/WT | – | – | – |
| UCD153 | Strain derived from ATCC 29133 | – | – | High rate of conjugal transfer, no hormogonia differentiation |
| Δ RR | Deletion of scytonemin TCR response regulator derived from UCD 153 | Npun_F1278 | DNA-binding transcription factor initiating transcription of scytonemin operon | Total abolition of scytonemin production |
| Δ Reg | Deletion of scytonemin response regulator and histidine kinase derived from UCD 153 | Npun_F1278, Npun_F1277 | Two component regulatory system controlling expression of the scytonemin operon | Total abolition of scytonemin production |
| Δ hcyA | Deletion of anti-sigma factor antagonist derived from ATCC 29133 | Npun_F1682 | Inhibitor of anti-sigma factor | Mild reduction in hormogonia differentiation under phototactic induction |
| Δ hcyC | Deletion of anti-sigma factor derived from ATCC 29133 | Npun_F1684 | Inhibitor of sigma factor | No reduction in hormogonia differentiation under phototactic induction |
| Δ σ J | Deletion of sigma factor J derived from ATCC 29133 | Npun_R1337 | Master regulator of phototactic hormogonia response | Total abolition of hormogonia response |

understanding. Our current interpretation was unexpectedly hampered by the discovery that strain UCD 153, which was used to derive the scyTCR mutants, was in fact deficient in hormogonia differentiation, which prevented us from further probing effects of its mutants on the phenotype directly. The interrogation of new mutant strains based on the ATCC 29133 strain, both targeting the scyTCR and other components shown by our study to be important in the hcy system, particularly *hcyD*, should prove useful in this respect. Additionally, further probing of environmental cues in various combinations may help clarify the precise conditions that bring about an increase in fitness to *Nostoc*, and perhaps also other similar genera of cyanobacteria, by fleeing UV-A exposure via developmental processes, in that currently this outcome occurs under exposure to UV-A alone (with no exposure to visible light), a situation that does not happen in nature. In this regard, it is useful to be reminded of the limitations of using model laboratory strains kept for decades under laboratory conditions to interpret situations in their original habitat, in that they are released from the selective pressures that honed adaptations of fitness value there, as the case of strain UCD 153 most poignantly reminds us.

STAR★METHODS

Detailed methods are provided in the online version of this paper and include the following:

- KEY RESOURCES TABLE
- RESOURCE AVAILABILITY
 - Lead contact
 - Materials availability
 - Data and code availability
- EXPERIMENTAL MODEL AND SUBJECT DETAILS
- METHOD DETAILS
 - Phenotypic characterization
 - RNA extraction, sequencing and RNAseq analyses
 - Targeted analysis by RT-qPCR
 - Bacterial adenylate cyclase two-hybrid assays
- QUANTIFICATION AND STATISTICAL ANALYSES

SUPPLEMENTAL INFORMATION

Supplemental information can be found online at <https://doi.org/10.1016/j.isci.2022.104361>.

ACKNOWLEDGMENTS

Funding for this research included NSF Award #1858551, Regulation of microbial sunscreen biosynthesis, to FG-P, and NSF award #1753690, Characterization of the gene regulatory network promoting hormogonium development, to DDR.

AUTHOR CONTRIBUTIONS

KK conducted phenotypic characterizations, RNAseq and bioinformatic analyses. DF and DR constructed mutants. KK and FG-P wrote manuscript and prepared figures. All authors evaluated results and revised manuscript.

DECLARATION OF INTERESTS

The authors declare no competing interests resource availability.

Received: June 1, 2021

Revised: January 17, 2022

Accepted: May 2, 2022

Published: June 17, 2022

REFERENCES

- Ackermann, M. (2015). A functional perspective on phenotypic heterogeneity in microorganisms. *Nat. Rev. Microbiol.* 13, 497–508. <https://doi.org/10.1038/nrmicro3491>.
- Adams, D.G. (2000). Heterocyst formation in cyanobacteria. *Curr. Opin. Microbiol.* 3, 618–624. [https://doi.org/10.1016/S1369-5274\(00\)00150-8](https://doi.org/10.1016/S1369-5274(00)00150-8).
- Armstrong, R.E., Hayes, P.K., and Walsby, A.E. (1983). Gas vacuole formation in hormogonia of *Nostoc muscorum*. *Microbiology* 129, 263–270. <https://doi.org/10.1099/00221287-129-2-263>.
- Avery, S.V. (2006). Microbial cell individuality and the underlying sources of heterogeneity. *Nat. Rev. Microbiol.* 4, 577–587. <https://doi.org/10.1038/nrmicro1460>.
- Battesti, A., and Bouveret, E. (2012). The bacterial two-hybrid system based on adenylate cyclase reconstitution in *Escherichia coli*. *Methods* 58, 325–334. <https://doi.org/10.1016/j.ymeth.2012.07.018>.
- Beaumont, H.J.E., Gallie, J., Kost, C., Ferguson, G.C., and Rainey, P.B. (2009). Experimental evolution of bet hedging. *Nature* 462, 90–93. <https://doi.org/10.1038/nature08504>.
- Bebout, B.M., and Garcia-Pichel, F. (1995). UV B-induced vertical migrations of cyanobacteria in a microbial mat. *Appl. Environ. Microbiol.* 61, 4215–4222. <https://doi.org/10.1128/aem.61.12.4215-4222.1995>.
- Bertani, G. (1959). Sensitivities of different bacteriophage species to ionizing radiation. *J. Bacteriol.* 79, 387–393.
- Cai, Y.P., and Wolk, C.P. (1990). Use of a conditionally lethal gene in *Anabaena* sp. strain PCC 7120 to select for double recombinants and to entrap insertion sequences. *J. Bacteriol.* 172, 3138–3145. <https://doi.org/10.1128/jb.172.6.3138-3145.1990>.
- Campbell, E.L., Christman, H., and Meeks, J.C. (2008). DNA microarray comparisons of plant factor and nitrogen deprivation-induced hormogonia reveal decision-making transcriptional regulation patterns in *Nostoc punctiforme*. *J. Bacteriol.* 190, 7382–7391. <https://doi.org/10.1128/JB.00990-08>.
- Campbell, E.L., Summers, M.L., Christman, H., Martin, M.E., and Meeks, J.C. (2007a). Global gene expression patterns of *Nostoc punctiforme* in steady-state dinitrogen-grown heterocyst-containing cultures and at single time points during the differentiation of akinetes and hormogonia. *J. Bacteriol.* 189, 5247–5256. <https://doi.org/10.1128/JB.00360-07>.
- Campbell, E.L., Summers, M.L., Christman, H., Martin, M.E., and Meeks, J.C. (2007b). Global gene expression patterns of *Nostoc punctiforme* in steady-state dinitrogen-grown heterocyst-containing cultures and at single time points during the differentiation of akinetes and hormogonia. *J. Bacteriol.* 189, 5247–5256. <https://doi.org/10.1128/JB.00360-07>.
- Castenholz, R.W., and Garcia-Pichel, F. (2007). Cyanobacterial responses to UV-radiation. *Ecol. Cyanobacteria* 21, 591–611. <https://doi.org/10.7551/mitpress/1247.003.0035>.
- Cohen, M.F., Wallis, J.G., Campbell, E.L., and Meeks, J.C. (1994). Transposon mutagenesis of *Nostoc* sp. strain ATCC 29133, a filamentous cyanobacterium with multiple cellular differentiation alternatives. *Microbiology* 140, 3233–3240. <https://doi.org/10.1099/13500872-140-12-3233>.
- Davis, M.C., Kesthely, C.A., Franklin, E.A., and MacLellan, S.R. (2017). The essential activities of the bacterial sigma factor. *Can. J. Microbiol.* 63, 89–99. <https://doi.org/10.1139/cjm-2016-0576>.
- De Jong, I.G., Haccou, P., and Kuipers, O.P. (2011). Bet hedging or not? A guide to proper classification of microbial survival strategies. *BioEssays* 33, 215–223. <https://doi.org/10.1002/bies.201000127>.
- Delumeau, O., Dutta, S., Brigulla, M., Kuhnke, G., Hardwick, S.W., Völker, U., Yuckin, M.D., and Lewis, R.J. (2004). Functional and structural characterization of RsbU, a stress signaling protein phosphatase 2C. *J. Biol. Chem.* 279, 40927–40937. <https://doi.org/10.1074/jbc.M405464200>.
- Dodds, W.K., Gudder, D.A., and Mollenhauer, D. (1995). The ecology of *Nostoc*. *J. Phycol.* 31, 2–18. <https://doi.org/10.1111/j.0022-3646.1995.00002.x>.
- Ekman, M., Picossi, S., Campbell, E.L., Meeks, J.C., and Flores, E. (2013). A *Nostoc punctiforme* sugar transporter necessary to establish a cyanobacterium-plant symbiosis. *Plant. Physiol.* 161, 1984–1992. <https://doi.org/10.1104/pp.112.213116>.
- Ferreira, D., and Garcia-Pichel, F. (2016). Mutational studies of putative biosynthetic genes for the cyanobacterial sunscreen scytonemin in *Nostoc punctiforme* ATCC 29133. *Front. Microbiol.* 7, 1–10. <https://doi.org/10.3389/fmicb.2016.00735>.
- Gao, Q., and Garcia-Pichel, F. (2011). Microbial ultraviolet sunscreens. *Nat. Rev. Microbiol.* 9, 791–802. <https://doi.org/10.1038/nrmicro2649>.
- Gao, R., and Stock, A.M. (2009). Biological insights from structures of two-component proteins. *Annu. Rev. Microbiol.* 63, 133–154. <https://doi.org/10.1146/annurev.micro.091208.073214>.
- Garcia-Pichel, F., and Castenholz, R.W. (1991). Characterization and biological implications of scytonemin, a cyanobacterial sheath. *J. Phycol.* 27, 395–409. <https://doi.org/10.1111/j.0022-3646.1991.00395.x>.
- Gonzalez, A., Riley, K.W., Harwood, T.V., Zuniga, E.G., Risser, D.D., and Ellermeier, C.D. (2019). A tripartite, hierarchical sigma factor cascade promotes hormogonium development in the filamentous cyanobacterium *Nostoc punctiforme*. *Nostoc punctiforme* 4. e00231–19. <https://doi.org/10.1128/mSphere.00231-19>.
- Helmann, J.D., and Chamberlin, M.J. (1988). Structure and function of bacterial sigma factors.

- Annu. Rev. Biochem. 57, 839–872. <https://doi.org/10.1146/annurev.bi.57.070188.004203>.
- Holland, S.L., Reader, T., Dyer, P.S., and Avery, S.V. (2014a). Phenotypic heterogeneity is a selected trait in natural yeast populations subject to environmental stress. *Environ. Microbiol.* 16, 1729–1740. <https://doi.org/10.1111/1462-2920.12243>.
- Holland, S.L., Reader, T., Dyer, P.S., and Avery, S.V. (2014b). Phenotypic heterogeneity is a selected trait in natural yeast populations subject to environmental stress. *Environ. Microbiol.* 16, 1729–1740. <https://doi.org/10.1111/1462-2920.12243>.
- Karimova, G., Pidoux, J., Ullmann, A., and Ladant, D. (1998). A bacterial two-hybrid system based on a reconstituted signal transduction pathway. *Proc. Natl. Acad. Sci. U S A.* 95, 5752–5756. <https://doi.org/10.1073/pnas.95.10.5752>.
- Khayatan, B., Meeks, J.C., and Risser, D.D. (2015). Evidence that a modified type IV pilus-like system powers gliding motility and polysaccharide secretion in filamentous cyanobacteria. *Mol. Microbiol.* 98, 1021–1036. <https://doi.org/10.1111/mmi.13205>.
- Klicki, K., Ferreira, D., Hamill, D., Dirks, B., Mitchell, N., and Garcia-Pichel, F. (2018). The widely conserved ebo cluster is involved in precursor transport to the periplasm during scytonemin synthesis in *Nostoc punctiforme*. *MBio* 9, e02266–18. <https://doi.org/10.1128/mBio.02266-18>.
- Kolde, R., and Antoine, L. (2015). Pheatmap: Pretty Heatmaps. <https://github.com/raivokolde/pheatmap>.
- Levy, S.F., Ziv, N., and Segal, M.L. (2012). Bet hedging in yeast by heterogeneous, age-correlated expression of a stress protectant. *PLoS Biol.* 10, 1001325. <https://doi.org/10.1371/journal.pbio.1001325>.
- Magasanik, B. (1961). Catabolite repression. *Cold. Spring. Harb. Symp. Quant. Biol.* 26, 249–256. <https://doi.org/10.1101/SQB.1961.026.01.031>.
- Marchler-Bauer, A., Bo, Y., Han, L., He, J., Lanczycki, C.J., Lu, S., Chitsaz, F., Derbyshire, M.K., Geer, R.C., Gonzales, N.R., et al. (2017). CDD/SPARCLE: functional classification of proteins via subfamily domain architectures. *Nucleic. Acids. Res.* 45, D200–D203. <https://doi.org/10.1093/nar/gkw1129>.
- Marchler-Bauer, A., Derbyshire, M.K., Gonzales, N.R., Lu, S., Chitsaz, F., Geer, L.Y., Geer, R.C., He, J., Gwadz, M., Hurwitz, D.I., et al. (2015). CDD: NCBI's conserved domain database. *Nucleic Acids Res.* 43, D222–D226. <https://doi.org/10.1093/nar/gku1221>.
- Marchler-Bauer, A., Lu, S., Anderson, J.B., Chitsaz, F., Derbyshire, M.K., DeWeese-Scott, C., Fong, J.H., Geer, L.Y., Geer, R.C., Gonzales, N.R., et al. (2011). CDD: a Conserved Domain Database for the functional annotation of proteins. *Nucleic Acids Res.* 39, D225–D229. <https://doi.org/10.1093/nar/gkq1189>.
- Marsac, N.T. (1994). Differentiation of hormogonia and relationships with other biological processes. In *The Molecular Biology of Cyanobacteria* (Springer), pp. 825–842. https://doi.org/10.1007/978-94-011-0227-8_28.
- McCaw, M.L., Lykken, G.L., Singh, P.K., and Yahr, T.L. (2002). ExsD is a negative regulator of the *Pseudomonas aeruginosa* type III secretion regulon. *Mol. Microbiol.* 46, 1123–1133. <https://doi.org/10.1046/j.1365-2958.2002.03228.x>.
- Meeks, J., Campbell, E., Summers, M., and Wong, F. (2002). Cellular differentiation in the cyanobacterium *Nostoc punctiforme*. *Arch. Microbiol.* 178, 395–403. <https://doi.org/10.1007/s00203-002-0476-5>.
- Meeks, J.C., Elhai, J., Thiel, T., Potts, M., Larimer, F., Lamerdin, J., Predki, P., and Atlas, R. (2001). An overview of the Genome of *Nostoc punctiforme*, a multicellular, symbiotic Cyanobacterium. *Photosyn. Res.* 70, 85–106. <https://doi.org/10.1023/A:1013840025518>.
- Mercer, R.G., and Lang, A.S. (2014). Identification of a predicted partner-switching system that affects production of the gene transfer agent RcGTA and stationary phase viability in *Rhodobacter capsulatus*. *BMC. Microbiol.* 14, 1–6. <https://doi.org/10.1186/1471-2180-14-71>.
- Mohr, W., Vagner, T., Kuypers, M.M.M., Ackermann, M., and LaRoche, J. (2013). Resolution of conflicting signals at the single-cell level in the regulation of cyanobacterial photosynthesis and nitrogen fixation. *PLoS One* 8, e66060. <https://doi.org/10.1371/journal.pone.0066060>.
- Morris, A.R., and Visick, K.L. (2013). The response regulator SypE controls biofilm formation and colonization through phosphorylation of the syp-encoded regulator SypA in *Vibrio fischeri*. *Mol. Microbiol.* 87, 509–525. <https://doi.org/10.1111/mmi.12109>.
- Nadeau, T., Howard-Williams, C., and Castenholz, R. (1999). Effects of solar UV and visible irradiance on photosynthesis and vertical migration of *Oscillatoria* sp. (Cyanobacteria) in an Antarctic microbial mat. *Aquat. Microb. Ecol.* 20, 231–243. <https://doi.org/10.3354/ame020231>.
- Naurin, S., Bennett, J., Videau, P., Philmus, B., and Soule, T. (2016). The response regulator Npun_F1278 is essential for scytonemin biosynthesis in the cyanobacterium *Nostoc punctiforme* ATCC 29133. *J. Phycol.* 52, 564–571. <https://doi.org/10.1111/jpy.12414>.
- Potts, M. (1994). Desiccation tolerance of prokaryotes. *Microbiol. Rev.* 58, 755–805. <https://doi.org/10.1128/mmr.58.4.755-805.1994>.
- Raj, A., and van Oudenaarden, A. (2008). Nature, nurture, or chance: stochastic gene expression and its consequences. *Cellule* 135, 216–226. <https://doi.org/10.1016/j.cell.2008.09.050>.
- Rajeev, L., Luning, E.G., Dehal, P.S., Price, M.N., Arkin, A.P., and Mukhopadhyay, A. (2011). Systematic mapping of two component response regulators to gene targets in a model sulfate reducing bacterium. *Genome. Biol.* 12, R99. <https://doi.org/10.1186/gb-2011-12-10-r99>.
- Rastogi, R.P., Sinha, R.P., Moh, S.H., Lee, T.K., Kottuparambil, S., Kim, Y.-J., Rhee, J.-S., Choi, E.-M., Brown, M.T., Häder, D.-P., and Han, T. (2014). Ultraviolet radiation and cyanobacteria. *J. Photochem. Photobiol. B Biol.* 141, 154–169. <https://doi.org/10.1016/j.jphotobiol.2014.09.020>.
- Revsbech, N.P., and Jorgensen, B.B. (1983). Photosynthesis of benthic microflora measured with high spatial resolution by the oxygen microprofile method: capabilities and limitations of the method. *Limnol. Oceanogr.* 28, 749–756. <https://doi.org/10.4319/lo.1983.28.4.0749>.
- Riley, K.W., Gonzalez, A., and Risser, D.D. (2018). A partner-switching regulatory system controls hormogonium development in the filamentous cyanobacterium *Nostoc punctiforme*. *Mol. Microbiol.* 109, 555–569. <https://doi.org/10.1111/mmi.14061>.
- Risser, D.D., Chew, W.G., and Meeks, J.C. (2014). Genetic characterization of the hmp locus, a chemotaxis-like gene cluster that regulates hormogonium development and motility in *Nostoc punctiforme*. *Mol. Microbiol.* 92, 222–233. <https://doi.org/10.1111/mmi.12552>.
- Schurr, M.J., Martin, D.W., Mudd, M.H., Hibler, N.S., Boucher, J.C., and Deretic, V. (1993). The algD promoter: regulation of alginate production by *Pseudomonas aeruginosa* in cystic fibrosis. *Cell. Mol. Biol. Res.* 39, 371–376.
- Singh, S.P., Hä Der, D.-P., and Sinha, R.P. (2010). Cyanobacteria and ultraviolet radiation (UVR) stress: mitigation strategies. *Ageing. Res. Rev.* 9, 79–90. <https://doi.org/10.1016/j.arr.2009.05.004>.
- Smits, W.K., Kuipers, O.P., and Veening, J.W. (2006). Phenotypic variation in bacteria: the role of feedback regulation. *Nat. Rev. Microbiol.* 4, 259–271. <https://doi.org/10.1038/nrmicro1381>.
- Song, J.-Y., Cho, H.S., Cho, J.-I., Jeon, J.-S., Lagarias, J.C., and Park, Y.-I. (2011). Near-UV cyanobacteriochrome signaling system elicits negative phototaxis in the cyanobacterium *Synechocystis* sp. PCC 6803. *Proc. Natl. Acad. Sci.* 108, 10780–10785. <https://doi.org/10.1073/PNAS.1104242108>.
- Soule, T., Gao, Q., Stout, V., and Garcia-pichel, F. (2013). The global response of *nostoc punctiforme* ATCC 29133 to UVA stress, assessed in a temporal DNA microarray study. *Photochem. Photobiol.* 89, 415–423. <https://doi.org/10.1111/php.12014>.
- Soule, T., Garcia-Pichel, F., and Stout, V. (2009a). Gene expression patterns associated with the biosynthesis of the sunscreen scytonemin in *Nostoc punctiforme* ATCC 29133 in response to UVA radiation. *J. Bacteriol.* 191, 4639–4646. <https://doi.org/10.1128/JB.00134-09>.
- Soule, T., Palmer, K., Gao, Q., Potrafka, R.M., Stout, V., and Garcia-Pichel, F. (2009b). A comparative genomics approach to understanding the biosynthesis of the sunscreen scytonemin in cyanobacteria. *BMC. Genomics.* 10, 336. <https://doi.org/10.1186/1471-2164-10-336>.
- Soule, T., Stout, V., Swingle, W.D., Meeks, J.C., and Garcia-Pichel, F. (2007). Molecular genetics and genomic analysis of scytonemin biosynthesis in *Nostoc punctiforme* ATCC 29133. *J. Bacteriol.* 189, 4465–4472. <https://doi.org/10.1128/JB.01816-06>.
- Spitt, S.D., and Risser, D.D. (2016). The non-metabolizable sucrose analog sucralose is a potent inhibitor of hormogonium differentiation

in the filamentous cyanobacterium *Nostoc punctiforme*. *Arch. Microbiol.* 198, 137–147. <https://doi.org/10.1007/s00203-015-1171-7>.

Tjaden, B. (2015). De novo assembly of bacterial transcriptomes from RNA-seq data. *Genome Biol.* 16, 1. <https://doi.org/10.1186/s13059-014-0572-2>.

van Gernerden, H. (1993). Microbial mats: a joint venture. *Mar. Geol.* 113, 3–25. [https://doi.org/10.1016/0025-3227\(93\)90146-M](https://doi.org/10.1016/0025-3227(93)90146-M).

Wagner, J.R., Brunzelle, J.S., Forest, K.T., and Vierstra, R.D. (2005). A light-sensing knot revealed by the structure of the chromophore-binding domain of phytochrome. *Nature* 438, 325–331. <https://doi.org/10.1038/nature04118>.

Whitton, B.A., and Potts, M. (2012). Introduction to the cyanobacteria. In *Ecol. Cyanobacteria II Their Divers. Sp. Time*. https://doi.org/10.1007/978-94-007-3855-3_1.

Wiltbank, L.B., and Kehoe, D.M. (2019). Diverse light responses of cyanobacteria mediated by phytochrome superfamily photoreceptors. *Nat. Rev. Microbiol.* 17, 37–50. <https://doi.org/10.1038/s41579-018-0110-4>.

Wösten, M.M.S.M. (1998). Eubacterial sigma-factors. *FEMS. Microbiol. Rev.* 22, 127–150. <https://doi.org/10.1111/j.1574-6976.1998.tb00364.x>.

STAR★METHODS

KEY RESOURCES TABLE

| REAGENT or RESOURCE | SOURCE | IDENTIFIER |
|--|---|---|
| Bacterial and virus strains | | |
| <i>Nostoc punctiforme</i> ATCC 29133 | ATCC | N/A |
| <i>Nostoc punctiforme</i> UCD153 | U. California, Davis (Campbell et al., 2007) | https://doi.org/10.1128/JB.00990-08 |
| <i>Nostoc punctiforme</i> UCD153 ΔRR | This work | N/A |
| <i>Nostoc punctiforme</i> UCD153 ΔReg | This work | N/A |
| <i>Nostoc punctiforme</i> ATCC29133 ΔhcyA | This work | N/A |
| <i>Nostoc punctiforme</i> ATCC29133 ΔhcyC | This work | N/A |
| <i>Nostoc punctiforme</i> ATCC29133 ΔσJ | U of the Pacific (Gonzalez et al., 2019) | https://doi.org/10.1128/mSphere.00231-19 |
| Oligonucleotides | | |
| <i>mpB</i> targeting sequence: TAAGAGCGCACCAGCAGTAT | This work | N/A |
| <i>gvpA</i> targeting sequence: TGACCGCATCTTGGACAAAGG | This work | N/A |
| <i>pilM</i> targeting sequence: CTAACGGATGAAGTGCGCCG | This work | N/A |
| <i>hcA</i> targeting sequence: ATATATCTAGATGTGAAAAATA AAATTTATCTAAAAGTCAA | This work | N/A |
| <i>hcyC</i> targeting sequence (two-hybrid assay): ATATAGGATCCCCCTACAAATGATTCATATTC | This work | N/A |
| <i>hcyC</i> targeting sequence (5'): ATATAGGATCCTC CTCGTCGATCCAATAATG | This work | N/A |
| <i>hcyC</i> targeting sequence (3'): CACAGACCTTTACTATT AATCCTCTTATCTAAGTTTTG | This work | N/A |
| <i>hcyC</i> targeting sequence (5'): ATATAGGATCCCCC TACAAATGATTCATATTC | This work | N/A |
| <i>hcyA</i> targeting sequence (3'): CCATGAGCATTACACAGT AAGTTCCTAGACTAG | This work | N/A |
| <i>hcyA</i> targeting sequence (5'): ATATAGGATCCCCCTAC AAATGATTCATATTC | This work | N/A |
| <i>ScyRR</i> targeting sequence: GTGGAGGATCCGTCT ATTTTTGTATTCCTC | This work | N/A |
| <i>ScyTCR</i> targeting sequence: GTGGACGGATCCCAAA GGCTGGCCATTGC | This work | N/A |
| Recombinant DNA | | |
| Plasmid pDDR415 [pRL278::ΔNpF1682 (BamHI-SacI)] | This work | N/A |
| Plasmid pDDR417 [pRL278::ΔNpF1684 (BamHI-SacI)] | This work | N/A |
| Plasmid pDDR437 [pKT25::NpF1684 (XbaI-KpnI)] | This work | N/A |
| Plasmid pDPF1278 [pRL278::ΔNpF1278-1277 (BamHI-SacI)] | This work | N/A |
| Plasmid pDDR435 [pUT18c::NpF1682 S49A (XbaI-KpnI)] | Riley et al., 2018 | https://doi.org/10.1111/mmi.14061 |
| Plasmid pDPF1277 [pRL278::ΔNpF1278-1277 (BamHI-SacI)] | This work | N/A |
| Plasmid pDPF1278 [pRL278::ΔNpF1278-1277 (BamHI-SacI)] | This work | N/A |
| Plasmid pDDR415 [pRL278::ΔNpF1682 (BamHI-SacI)] | Riley et al. (2018) | https://doi.org/10.1111/mmi.14061 |

RESOURCE AVAILABILITY

Lead contact

Further information and requests for resources and reagents should be directed to and will be fulfilled by the lead contact, Ferran Garcia-Pichel (ferran@asu.edu).

Materials availability

Mutant strains, natural variants and plasmids used in this work are freely available directly from the lead contact upon request. The wild-type strain is also available from the American Type Culture Collection. There are no newly developed reagents associated with this work.

Data and code availability

Sequence datasets generated in this study are available at NCBI's SRA database with accession number PRJNA728749. No new code resources were used in this research. Other phenotypic or analytical data are available in the manuscript in graphical or photographic form. Any additional information and source data, when applicable, is available on request from the corresponding author.

EXPERIMENTAL MODEL AND SUBJECT DETAILS

RNA sequencing experiments were conducted with a spontaneous derivative strain of *Nostoc punctiforme* ATCC 29133 (PCC 73102), UCD 153, that displays dispersed growth and a higher frequency of gene replacement by conjugal transfer ([Campbell et al., 2007b](#)). Mutant strains ΔReg and ΔRR , with complete (Npun_F1278 and Npun_F1277) or partial (Npun_F1278) deletions in the scytonemin TCR, were derived from it. Hormogonia induction experiments were carried out with the original wild-type, *Nostoc punctiforme* strain ATCC 29133, because UCD 153 does not exhibit phototactic hormogonia induction. Deletion mutant $\Delta sigJ$, $\Delta hcyA$ and $\Delta hcyC$ were derived from ATCC 29133. All strains were grown as previously described ([Ferreira and Garcia-Pichel, 2016](#)) in liquid Allen and Arnon (AA) medium, diluted 4-fold (AA/4), and on solidified AA medium plates under white light at 50 $\mu\text{mol photons m}^{-2}\text{s}^{-1}$ at room temperature. Neomycin was used at 25 $\mu\text{g mL}^{-1}$ for the selection and maintenance of transformed single recombinants ([Bertani, 1959](#)). A detailed compilation of all strains used in this work is provided in [Table 1](#).

METHOD DETAILS

Phenotypic characterization

Scytonemin induction assays

Scytonemin production was induced by growing the strains in 15 × 100 mm glass Petri dishes under white light at 50 $\mu\text{mol photons m}^{-2}\text{s}^{-1}$ supplemented with a UV-A flux of 7.5 $\mu\text{mol photons m}^{-2}\text{s}^{-1}$ supplied by black-light fluorescent bulbs (General Electric) for 5 days at 21 °C. For some experiments, as noted where applicable, white light was omitted. Scytonemin production was detected by microscopic observation first, using a Carl Zeiss Axioscope.A1 at 100× magnification and by HPLC on a Waters e2695 equipped with a Supelco Discovery HS F5-5 column connected to a Waters 2998 PDA UV-Vis diode array detector as described in [Klicki et al., \(2018\)](#).

Standard Hormogonia induction assays

Hormogonia induction was carried out following [Khayatan et al., \(2015\)](#): *Nostoc* strains were streaked onto agar-solidified medium supplemented with 5% sucrose and grown heterotrophically in the dark until punctate colonies formed. Colonies were then transferred to agar-solidified media lacking sucrose and exposed to 10 $\mu\text{mol photons m}^{-2}\text{s}^{-1}$ provided at a 90-degree angle. Formation of hormogonia was detected visually under the dissection scope. Plate motility assays were performed by transferring colonies grown on AA/4 supplemented with 10% sucralose to AA/4 containing 0.5% Noble agar ([Khayatan et al., 2015](#)). This assay yields a massive differentiation of filaments involving the large majority of existing filaments.

Hormogonia/scytonemin co-induction was carried out on solid AA medium using aluminum foil wrapped glass Petri plates provided with a side window, so that white light could enter at a 90-degree angle at an intensity of 10 $\mu\text{mol photons m}^{-2}\text{s}^{-1}$. UV-A radiation was concurrently delivered from a top window, after passing through a 400 nm cut-off short-pass optical filter (Edmund Optics) to remove any visible light produced by the UV-A bulbs. This was necessary because we found in pilot experiments that the additional vertically supplied visible light inhibited standard phototactic hormogonia induction. For analyses,

scytonemin/hormogonia co-induction cultures were transferred from agar plates to microscope slides using a scalpel and photographed on a Carl Zeiss AxioScope.A1 at 1000× magnification using an Axiocam 105 color camera. They were inspected for morphologically identifiable hormogonia, and for the typical extracellular coloration imparted by scytonemin. UV-A exclusive hormogonia induction was carried out by plating strains from liquid cultures on to solid AA medium and incubating under UV-A irradiation without supplemental PAR for 48–96 h. Hormogonia spreading was quantified by measuring the area occupied by initial colony biomass and the area swept out by whisks of hormogonia using the Carl Zeiss Zen 3.1 software, subtracting the former from the latter, and dividing the difference by the initial biomass area.

RNA extraction, sequencing and RNAseq analyses

Total RNA was extracted from appropriately incubated cultures (UV-A-induced or uninduced) of each test strain (wild type, ΔRR and ΔReg) by being flash frozen and subjected to lysis by bead beating, followed by precipitation with 4M lithium chloride 20 mM Tris and 10 mM EDTA followed by purification using a Qiagen RNeasy spin column kit (Campbell et al., 2007a). Ribodepletion, cDNA synthesis and subsequent RNA sequencing were performed at the Arizona State University Genomics Facility as follows. Four μg of total RNA was submitted to ribodepletion using the MICROBExpress Bacterial mRNA Enrichment Kit (Ambion). Directional cDNA libraries were synthesized using rRNA depleted samples. Three libraries per strain were multiplexed and treatments sequenced independently on an Illumina NextSeq 500 using a v2 2x75 pair end kit sequenced generating 76 base pair reads, obtaining on average $9,773,321 \pm 5,550,035$ reads per sample, excluding 16 and 23S rRNA genes. Sequences were aligned and assembled to the *Nostoc punctiforme* PCC 73102 genome using Rockhopper (Tjaden, 2015) on default parameters independently for each replicate. Differential expression between mutants and UV treatments was calculated using the DEseq algorithm in Rockhopper (Tjaden, 2015). Given the roughly 6000 non rRNA genes in the *N. punctiforme* genome, only transcripts whose differential expression had a q-value (a false discovery rate corrected p value) of less than 10^{-15} were considered significant for downstream analyses. Contiguous genes of known function that exhibited similar degrees of differential expression were considered to be co-regulated. Reads per kilobase million for each gene from the Rockhopper output were square root transformed to accentuate expressional differences over a broader dynamic range. Heatmaps were constructed using Pheatmap (Kolde and Antoine, 2015)

Targeted analysis by RT-qPCR

Five-hundred ng of total RNA was used to synthesize cDNA using the Protoscript first-strand cDNA synthesis kit and random hexamer primers (New England Biolabs) according to manufacturer's protocols. 1 μL of resulting cDNA was used as qPCR template. Transcripts were amplified using primer sets targeting specific genes as described in Table S1, using an ABI 7900 HT Real-time PCR system and PerfeCTa SYBR Fastmix according to manufacturer's protocols. Transcript level was quantified in three technical replicates of each treatment using the $2^{-\Delta\Delta CT}$ method with expression normalized relative to *rnpB* as previously done by Gonzalez et al., (2019), and results averaged per treatment.

Bacterial adenylate cyclase two-hybrid assays

The bacterial adenylate cyclase two-hybrid assay (BACTH) was employed to probe protein-protein interaction between HcyC (Npun_F1684) and HcyA (Npun_F1682) with the putative phosphorylated serine residues replaced with alanine, as well as sigma factors C, F, and J. To construct a plasmid encoding HcyC fused to the T25 fragment of *B. pertussis* adenylate cyclase for bacterial adenylate cyclase two-hybrid (BACTH) analysis (Battesti and Bouveret, 2012; Karimova et al., 1998), the coding region gene was amplified via PCR and cloned into pKT25 as an XbaI-KpnI fragment using restriction sites introduced on the primers. BTH101 (adenylate cyclase-deficient) *E. coli* strains transformed with appropriate plasmids were streaked onto Lysogeny Broth (LB) agar plates containing 100 $\mu\text{g}/\text{mL}$ Ampicillin and 50 $\mu\text{g}/\text{mL}$ Kanamycin, and incubated at 30 °C for 48 h. For each strain, 1 mL of LB containing 100 $\mu\text{g}/\text{mL}$ Ampicillin, 50 $\mu\text{g}/\text{mL}$ Kanamycin and 0.5 mM Isopropyl β -D-1-thiogalactopyranoside (IPTG) was inoculated with several colonies from the plate, and cultures were then incubated overnight at 30 °C with shaking at 230 rpm. Subsequently, 2 μL were taken from each overnight culture and spotted onto MacConkey agar plates containing 100 $\mu\text{g}/\text{mL}$ Ampicillin and 50 $\mu\text{g}/\text{mL}$ Kanamycin. Plates were incubated at 30 °C for 48 h prior to imaging.

QUANTIFICATION AND STATISTICAL ANALYSES

Replication for phenotypic analyses was at least 3, and statistical significance was assessed through t-tests. For transcriptomic analyses, and given the roughly 6000 non rRNA genes in the *N. punctiforme* genome, only transcripts whose differential expression had a q-value (a false discovery rate corrected p value) of less than 10^{-15} were considered significant for downstream analyses.